Journal of Applied Mechanics Vol.13, pp.745-752 (August 2010) JSCE

ALE Finite Volume Method for Free-Surface Bingham Plastic Fluids with General Curvilinear Coordinates

自由液面を有するビンガム塑性流体に対する移動一般座標系有限体積法

Katsuaki NAGAI* and Satoru USHIJIMA**
永井克明・牛島省

*Member, Master Course Dept. CERE, Kyoto Univ. (C-cluster, Kyoto 615-8540)
**Member, Prof. ACCMS, Kyoto Univ. (Yoshida-Honmachi, Sakyo-ku, Kyoto 606-8501)

A numerical prediction method has been proposed to predict Bingham plastic fluids with free-surface in a two-dimensional container. Since the linear relationships between stress tensors and strain rate tensors are not assumed for non-Newtonian fluids, the liquid motions are described with Cauchy momentum equations rather than Navier-Stokes equations. The profile of a liquid surface is represented with the two-dimensional curvilinear coordinates which are generated in each computational step on the basis of the Arbitrary Lagrangian-Eulerian (ALE) method. Since the volumes of the fluid cells are transiently changed in the physical space, the geometric conservation law is applied to the finite volume discretizations. As a result, it has been shown that the present method enables us to predict reasonably the Bingham plastic fluids with free-surface in a container.

Key Words : *Bingham plastic fluid, free-surface flow, curvilinear coordinate, finite volume method, ALE method, geometric conservation law*

1. Introduction

In general, Newtonian fluids are used in fluid calculations in hydraulic engineering. However, debris flows, mud flows and lava flows have a characteristic different from clear water and hence these are treated as non-Newtonian fluids. Furthermore, it is reported that liquefied soils have a characteristic of pseudo-plastic fluid. Thus, it is difficult to describe various flows in civil engineering as Newtonian fluid. In addition, since many kinds of flows in the nature have free-surface, it is important to reveal the characteristic of non-Newtonian fluid flows with free-surfaces.

In civil engineering, liquefied sand and fresh concrete, which are categorized as Bingham plastic fluids, are often treated as the representative of non-Newtonian fluids. Thus, the present study are focused on the Bingham plastic fluids having free-surface.

In the past studies, the VOF techniques, the MAC methods and ALE formulation are used to numerically predict the Bingham plastic flows with free-surface [1),2),3)]. In this paper, the ALE formulation has been selected in order to represent the free surface profiles correctly.

Meanwhile, in fluid flow calculations, the use of moving coordinates is sometimes essential, e.g. in flows with moving boundaries. Owing to the movement of the coordinate system, an additional equation has to be solved in addition to the conservation equations. This equation relates the change of the elementary control volume to the coordinate frame velocity and is hence called by Thomas et al. [4)] the 'geometric conservation law'.

In the present study, a new computational technique is proposed to predict the Bingham plastic fluids having free-surface. The profile of a liquid surface is represented with the two-dimensional curvilinear coordinates which are generated in each computational step on the basis of the ALE method. Since the vol-

umes of the fluid cells are transiently changed in the physical space, the geometric conservation law is applied to the finite volume discretizations. In order to confirm the applicability of the present computational technique, numerical simulations are performed for the free-surface flows in a container

2. Numerical Procedures

2.1 Basic Equations in Moving Curvilinear Coordinates

For incompressible non-Newtonian fluids, the set of equations describing conservation of mass, momentum and geometry in a moving coordinate frame reads respectively.

$$\int_{V_0} \rho \frac{\partial J}{\partial t} dV_0 + \int_{\partial V_0} \rho J (U_m - V_m) n_m dS_0 = 0 \quad (1)$$

$$\int_{V_0} \frac{\partial (J u_i)}{\partial t} dV_0 + \int_{\partial V_0} J (U_m - V_m) u_i n_m dS_0 = -\frac{1}{\rho} \int_{\partial V_0} J \frac{\partial \xi_m}{\partial x_i} p n_m dS_0 + \frac{1}{\rho} \int_{\partial V_0} J \frac{\partial \xi_m}{\partial x_j} \tau_{ij} n_m dS_0 + \int_{V_0} f_i J \, dV_0 \quad (2)$$

$$\int_{V_0} \frac{\partial J}{\partial t} dV_0 = \int_{\partial V_0} J V_m n_m dS_0 \quad (3)$$

Here, t, ρ, p, τ_{ij} and f_i are time, density of liquid, pressure, deviatoric stress tensor and body force component per unit mass in x_i direction, respectively. As indicated in **Fig.1**, the spatial coordinates in the physical space are represented by x_i while ξ_m denotes the spatial coordinates in the computational space which tracks the moving boundaries. J is a Jacobian of the transformation defined by

$$J = \frac{\partial x_1}{\partial \xi_1} \frac{\partial x_2}{\partial \xi_2} - \frac{\partial x_1}{\partial \xi_2} \frac{\partial x_2}{\partial \xi_1}. \quad (4)$$

V_0 is an arbitrary spatial region of the computational space and its size is constant regardless of the computational step. n_m is the component of unit normal vector on V_0. u_i is velocity component in x_i direction, and the contravariant velocity components U_m and V_m are derived from the velocity of the liquid and that of the cell face in the computational space:

$$U_m = u_i \frac{\partial \xi_m}{\partial x_i} \quad (5)$$

$$V_m = \frac{\partial x_i}{\partial t} \frac{\partial \xi_m}{\partial x_i} \quad (6)$$

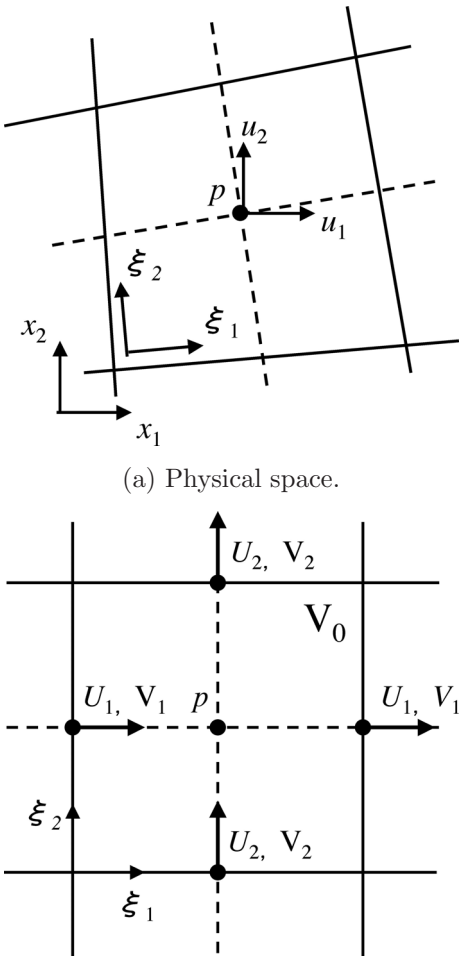

(a) Physical space.

(b) Computational space.

Fig. 1 Computational cell.

In the collocated grid system, proposed by Rhie and Chow [5], pressure and all velocity components are located at the cell-center points. In addition, cell-boundary velocity components are utilized in pressure calculation to prevent the velocity-pressure oscillation. On the other hand, the contravariant velocity components U_m and V_m are defined on the cell boundaries.

Eq. (3) is called the integral form of geometric conservation law, which represents that the volume change of a fluid cell is identified with the sum of the sweeping volume of each cell faces. The contravariant surface velocity component V_m has to satisfy the geometric conservation law [6]. The procedure will be outlined in the following section.

These conservation equations are discretized in the collocated grid system and solved with a finite volume method. On the basis of the computational method

for incompressible fluids [7], tentative velocity components are calculated at cell-center points with the Euler explicit method. The derived velocity components are spatially interpolated on the cell-boundaries and pressure computations are performed with C-HSMAC method [8].

2.2 Free-Surface Profile and Grid Generation

The kinematic boundary condition for the free surface is given by the following equation:

$$\frac{\partial h}{\partial t} = u_{s2} - u_{s1}\frac{\partial h}{\partial x_1} \tag{7}$$

where h is the free-surface height measured from a standard position and u_{si} is the velocity components of free surfaces. Eq. (7) can be discretized with the contravariant velocity components U_{s2} on the free-surface as

$$h^{n+1} = h^n + \frac{JU_{s2}^{n+1}\Delta\xi_1}{\Delta x_1}\Delta t. \tag{8}$$

Here, U_{s2}^{n+1} is obtained from the computational procedures in the C-HSMAC method [8].

The boundary profiles of fluids including free surface are used as the boundary conditions for grid generation. Under this boundary conditions, the following elliptic equation is employed to rearrange the internal grid points:

$$\frac{\partial}{\partial\xi_m}\left(\frac{\partial x_i}{\partial\xi_n}\frac{\partial\xi_n}{\partial x_j}\right)\frac{\partial\xi_m}{\partial x_j} + P_m\frac{\partial x_i}{\partial\xi_m} = 0 \tag{9}$$

Here, P_m is a user-defined function which allows us to control the mesh intervals in the physical space. The grid generation is performed at every computational step to represent the free-surface profiles.

The boundary conditions for velocity gradients $\partial u_{s1}/\partial\xi_2$ and $\partial u_{s2}/\partial\xi_2$ on the free surface are given by the relationships for normal stress and tangential stress [8].

2.3 Grid Velocity and Pressure Correction

In order to obtain the contravariant boundary velocity components V_m, we numerically solve Eq. (3). Eq. (3) is discretized with respect to time as the following form:

$$\int_{V_0}\frac{J^{n+1}-J^n}{\Delta t}dV_0 = \int_{\partial V_0} J^{n+1}V_m^{n+1}n_m dS_0 \tag{10}$$

where J^{n+1} are known quantities since the internal grid points have been rearranged. In addition, since the internal points move only in the x_2 direction in the present study, $V_1^n = 0$ at any computational step. Therefore, we can obtain V_2^{n+1} from Eq. (10).

Substituting Eq. (3) into Eq. (1), The mass conservation equation for the incompressible fluids reads

$$\int_{\partial V_0} J^{n+1}U_m^{n+1}n_m dS_0 = 0. \tag{11}$$

Using Eq. (11) instead of Eq. (1), the following Poisson equation for ϕ can be derived [8]:

$$\int_{\partial V_0} J^{n+1}g^{mj}\frac{\partial\phi}{\partial\xi_j}n_m dS_0 = \frac{\rho}{\Delta t}\int_{\partial V_0} J^{n+1}\hat{U}_{b,m}n_m dS_0 \tag{12}$$

with

$$g^{mj} = \frac{\partial\xi_m}{\partial x_k}\frac{\partial\xi_j}{\partial x_k} \tag{13}$$

and

$$\phi = p^{n+1} - p^n \tag{14}$$

where g^{mj} is a contravariant of the fundamental metric tensor, and $\hat{U}_{b,m}$ is the initial estimation of the contravariant velocity component.

When the numerical procedures in the C-HSMAC method is completed, p^{n+1} and U_m^{n+1} are established.

2.4 Bingham Model

In the Bingham model, the relationship between τ_{ij} and $\dot{\gamma}_{ij}$ is represented as follows:

$$\begin{cases} \tau_{ij} = \tau_0 + \eta_p\dot{\gamma}_{ij}, & |\tau| \geq \tau_0 \\ \dot{\gamma}_{ij} = 0, & |\tau| < \tau_0 \end{cases} \tag{15}$$

with

$$\dot{\gamma}_{ij} = \frac{\partial u_i}{\partial\xi_m}\frac{\partial\xi_m}{\partial x_j} + \frac{\partial u_j}{\partial\xi_m}\frac{\partial\xi_m}{\partial x_i} \tag{16}$$

where $\dot{\gamma}_{ij}$ is the rate of strain tensor. τ_0 and η_p represents yield stress and plastic viscosity respectively. $|\tau|$ is its second invariant and defined as following form:

$$|\tau| = \left[\frac{1}{2}\sum_{1\leq i,j\leq \dim}\tau_{ij}^2\right]^{\frac{1}{2}} \tag{17}$$

where dim is dimension number and equals 2 in this study. Eq. (17) means that Bingham plastic fluids exhibit no deformation at all (solid-like behavior) when the applied stress is below the yield stress, and that they flow like Newtonian fluids above the yield stress.

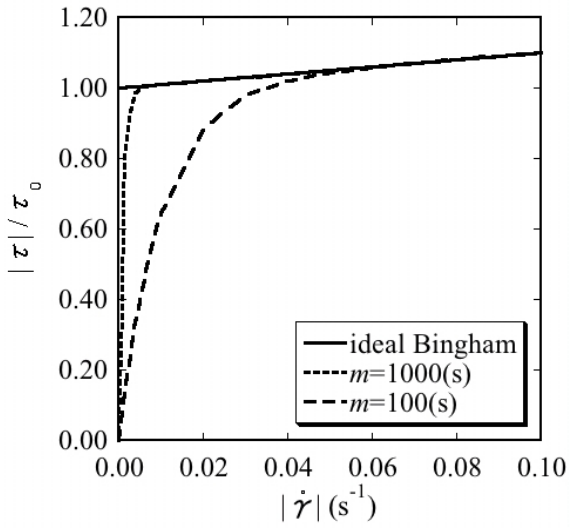

Fig. 2 Comparison with the Bingham model.

In the present analysis we decided to use the Papanastasiou model [9] which has the following form:

$$\tau_{ij} = \left[\eta_p + \frac{\tau_0}{|\dot{\gamma}|}(1 - e^{-m|\dot{\gamma}|})\right]\dot{\gamma}_{ij} \tag{18}$$

where m is the stress growth exponent. $|\dot{\gamma}|$ is its second invariant and defined as Eq. (17).

Fig.2 illustrates the relationship between the Bingham model and the Papanastasiou model. It is assumed that $\eta_p/\tau_0 = 1.0$(s) in **Fig.2**. For relatively large values of the exponent coefficient m, this model closely approximates the discontinuous Bingham behavior. The following calculations are performed using $m = 1000$(s).

Using shear-dependent viscosity η, τ_{ij} is related to $\dot{\gamma}_{ij}$ as follows:

$$\tau_{ij} = \eta\dot{\gamma}_{ij} \tag{19}$$

Comparing Eq. (18) with Eq. (19), we obtain the following form:

$$\eta(|\dot{\gamma}|) = \eta_p + \frac{\tau_0}{|\dot{\gamma}|}(1 - e^{-m|\dot{\gamma}|}) \tag{20}$$

η is calculated from Eq. (20) in each cell.

In the present analysis we use two dimensionless numbers. Bingham number Bn is defined as follows:

$$Bn = \frac{\tau_0 l}{\eta_p U} \tag{21}$$

where U and l are representative velocity and length respectively.

Reynolds number Re_{BI} is defined as follows:

$$Re_{BI} = \frac{\rho U l}{\eta_p} \tag{22}$$

3. Applicability of Prediction Method

3.1 Flow between two parallel plates

The flows between two parallel plates have been selected as a benchmark problem to validate the proposed computational method. The geometry and coordinates are shown in **Fig.3**, where the length L and width $2H$ are given by $L = 7.0$ and $2H = 1.0$ respectively. In addition, the non-slip condition is given on the plates. The velocity boundary conditions are $u_0 = 0.1$ at $x = 0$ and $\partial u/\partial x = 0$ at $x = L$. The pressure boundary conditions are $\partial p/\partial x = 0$ at $x = 0$ and $p = 0$ at $x = L$.

In order to confirm the numerical accuracy, the proposed method was applied in 30 × 20 non-uniform grid (**Fig.4**). The computational results at steady state are shown in **Fig.5**. The predicted velocity distribution in x direction agrees reasonably with the exact solution [10]. Thus, as shown in the previous study [11], it has been confirmed that the present computational techniques are applicable.

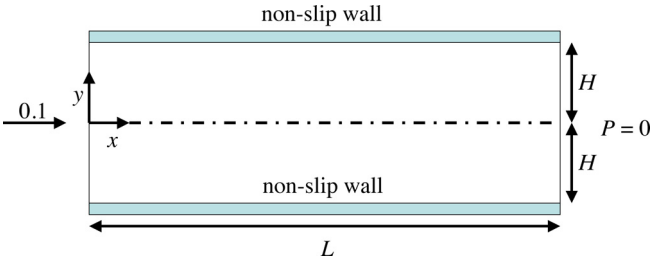

Fig. 3 The geometry of parallel plates and coordinates.

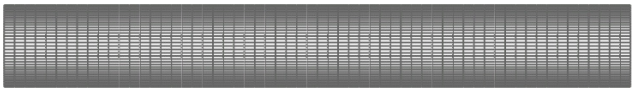

Fig. 4 Distribution of grid points.

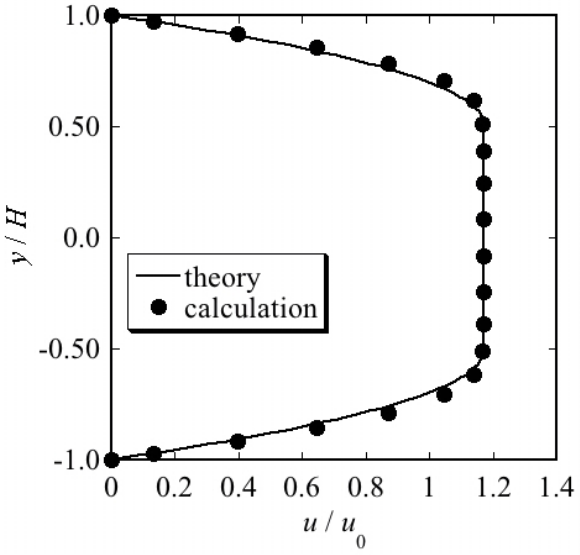

Fig. 5 Velocity distribution in x direction.

3.2 Free Oscillation

The numerical analysis of the free oscillation of the liquids with small and large amplitudes allows us to confirm that the numerical technique satisfies the basic specifications, such as free-surface boundary conditions and grid generation based on the ALE method. The two dimensional square container, as shown in **Fig.6**, is 1.0 × 1.0, in which the non-slip condition is given on all solid boundaries of the container. The gravity acts downward with 10.0 and the effect of surface tension is not taken into account. The initial profile of the free surface is given by

$$\eta = A\cos\left(\frac{\pi x}{l}\right) \tag{23}$$

where η is the liquid level on the basis of the still water depth h, l is the width of the container. The amplitude A equals 0.01 and the larger one is 0.1.

At first, the case of the free oscillation with a small amplitude was examined. **Fig.7** shows the time histories of the liquid level at $x = 0$ with the small amplitude for three computational results; one is a non-viscosity fluid, another is a Newton fluid ($Re = 40$) and the other is a Bingham plastic fluid ($Bn = 1.0$ and $Re = 100$). As shown in this figure, no numerical damping effects are found for non-viscosity fluid, which has a similar tendency to the previous study [8]. In addition, the adequate attenuation of the wave amplitudes is observed for the Newtonian fluid. On the other hand, the wave of the Bingham plastic fluid does not attenuate periodically and disappears within finite time. This suggests that the regions with various values of viscosity are distributed in the container. The characteristic of Bingham plastic fluids is qualitatively shown by the present method.

Besides, the numerical analysis of the free oscillation of Bingham plastic fluids with a large amplitude was performed. The generated computational grid distributions are shown in **Fig.8** and the predicted velocity vectors are presented in **Fig.9**. It can be seen that the adequate mesh regeneration is maintained and that the reasonable liquid motions are predicted in the calculation.

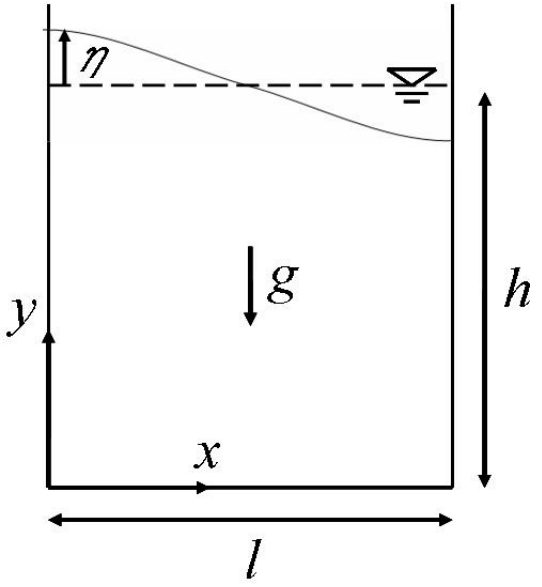

Fig. 6 Geometry of container and coordinates.

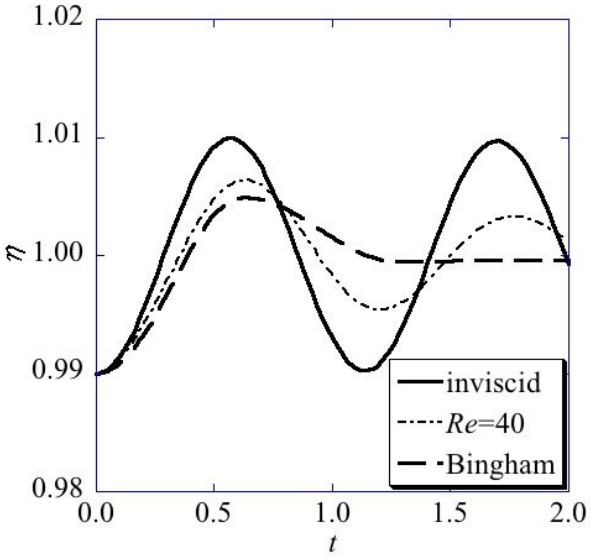

Fig. 7 Time histories of η at $x = 0$.

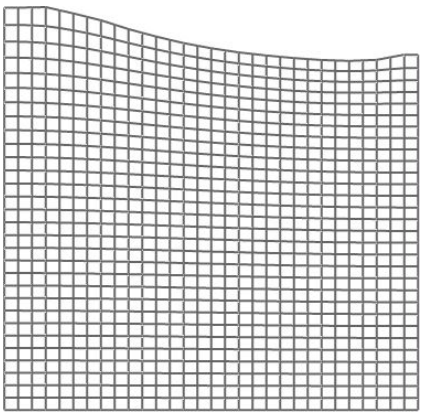

$t = 0.55$

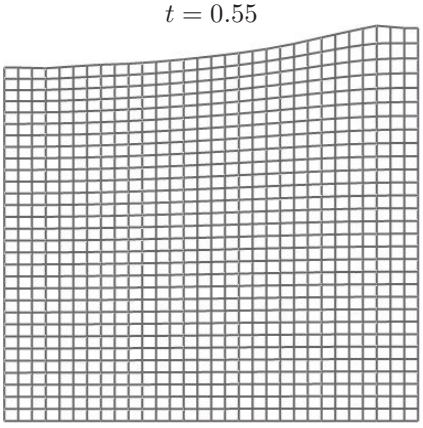

$t = 1.25$

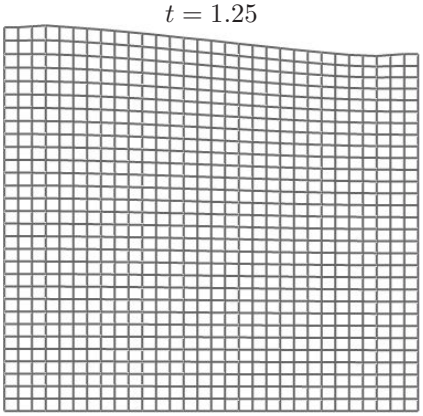

$t = 1.80$

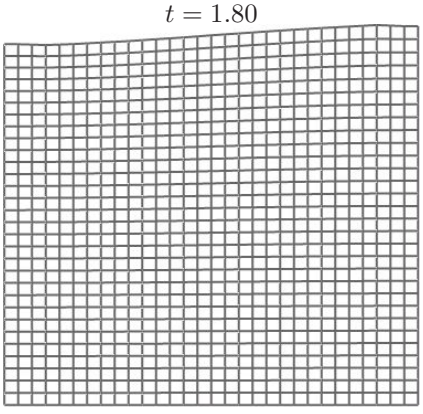

$t = 2.45$

Fig. 8 Generated curvilinear coordinates by ALE method.

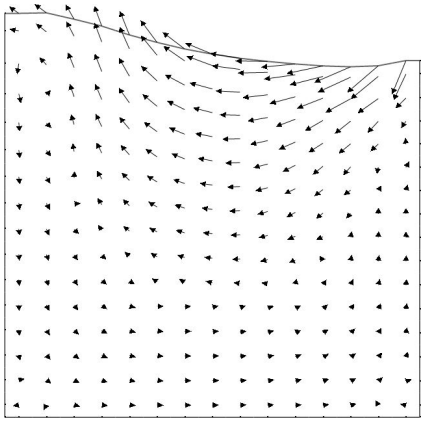

$t = 0.55$

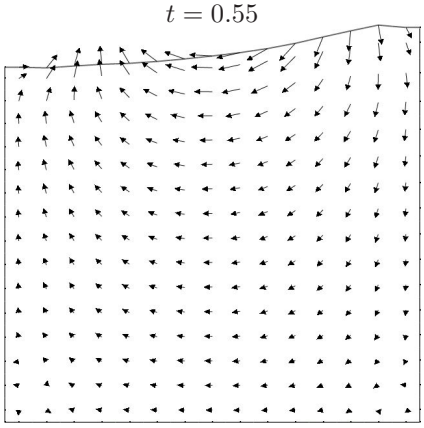

$t = 1.25$

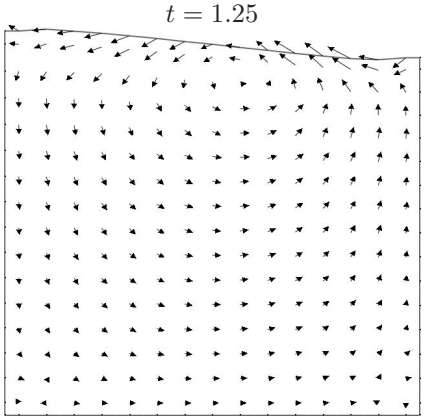

$t = 1.80$

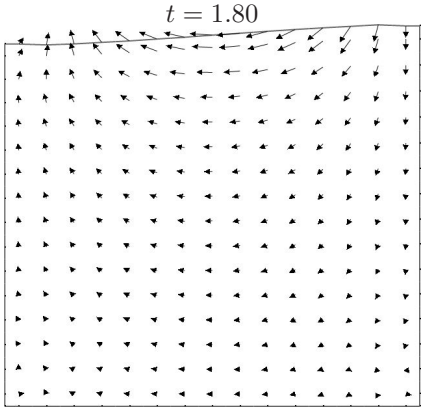

$t = 2.45$

Fig. 9 Computed velocity vectors and free surface profile with a large amplitude.

3.3 Lid-Driven Free-Surface Flow in a Container

The numerical analysis of free-surface profile in a container with moving bottom allows us to confirm that the present method is applicable to Newtonian fluids and Bingham plastic fluids with free surface.

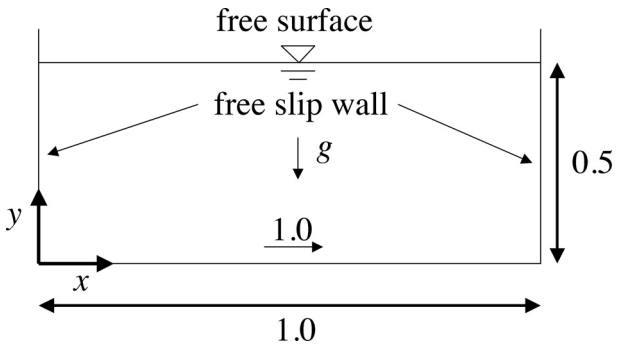

Fig. 10 Geometry of container and coordinates.

In a rectangular container with the width 1.0 and the average water depth 0.5, as shown **Fig.10**, the free-slip condition is given on both sides of the container, and the moving wall velocity equals 1.0. Reynolds number is 50, gravity force g is 10.0 and the effect of surface tension is not taken into account. Utilizing boundary-fitted coordinates, 15 × 15 non-uniform cells are generated.

Fig.11 shows the free-surface profile in steady state and the predicted velocity vectors are presented in **Fig.12**. The displacement of free-surface level of Bingham plastic fluids is smaller than that of Newtonian fluids.

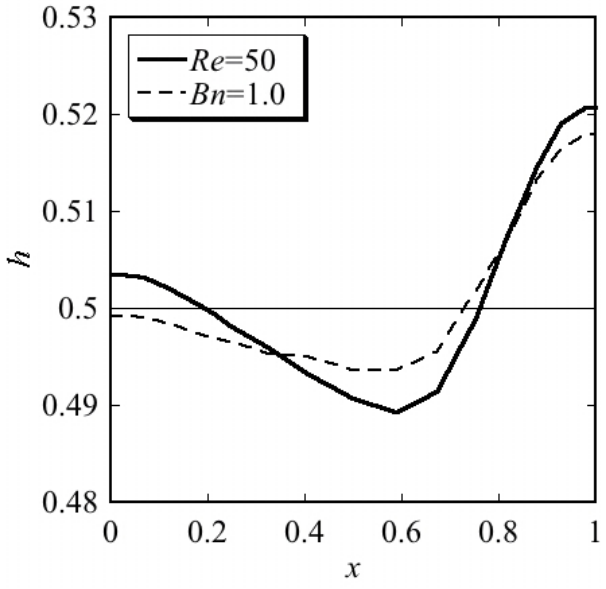

Fig. 11 Free surface profiles in steady state.

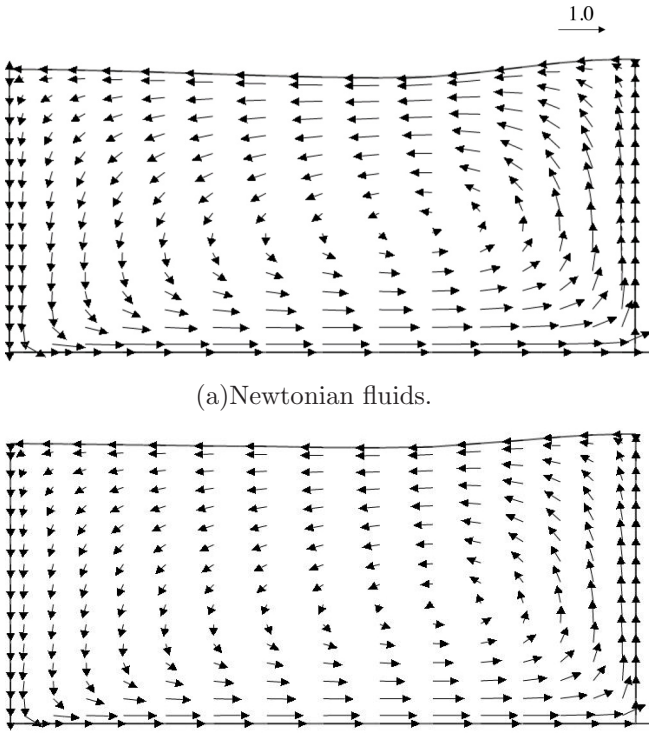

(a)Newtonian fluids.

(b)Bingham plastic fluids (Bn=1.0).

Fig. 12 Computed velocity vectors and free surface profiles.

4. Conclusions

A computational method has been proposed for free-surface Bingham plastic flows with general curvilinear coordinates by the ALE formulation. The transformed governing equations are discretized with a finite volume method in a collocated grid system. The stress tensors are described with the formulation proposed by Papanastaiou. Since the volumes of the fluid cells are transiently changed in the physical space, the geometric conservation law is accounted for in the discretization process.

In order to confirm the applicability of the present computational technique, numerical simulations have been conducted for the free oscillations and for lid-driven free-surface flows in a container. As a result, it has been proved that adequate solutions can be obtained for the free-surface Bingham plastic flows in a container. For the future works, we plan to compare the predicted results with experimental data and to confirm the applicability of the proposed method.

REFERENCES

1) H. T. Puay and T. Hosoda. Fundamental study of Bingham fluid by means of dam-break flow model. *Annual Hounal of hydraulic Engineering, JSCE*, Vol. 54, pp. 1177–1182, 2010.
2) T. Kokado, T. Hosoda, and T. Miyagawa. Study on a method of obtaining rheological coefficients of high-flow concrete with numerical analysys. *Journals of JSCE*, Vol. 648/V-47, pp. 109–125, 2000.
3) J. Étienne, E. J. Hinch, and J. Li. A lagransian-eulerian approach for the numerical simulation of free-surface flow of a viscoelastic material. *J. Non-Newtonian Fluid Mech.*, Vol. 136, pp. 157–166, 2006.
4) P. D. Thomas and C. K. Lombard. Geometric conservation law and its application to flow computations on moving grids. *AIAA Journal*, Vol. 17, pp. 1030–1037, 1979.
5) C. M. Rhie and W. L. Chow. Numerical study of the turbulent flow past an airfoil with trailing edge separation. *AIAA Journal*, Vol. 21, pp. 1525–1532, 1983.
6) I. Demirdžić and M. Perić. Space conservation law in finite volume calculations of fluid flow. *International Journal for Numerical Methods in Fluids*, Vol. 8, pp. 1037–1050, 1988.
7) S. Ushijima, M. Takemura, and I. Nezu. Investigation on computational schemes for MAC methods with collocated grid system. *Journals of JSCE*, No. 719/II-61, pp. 11–19, 2002.
8) S. Ushijima and I. Nezu. Computaional method for free-surface flows on collocated grid with moving curvilinear coordinates. *Journals of JSCE*, No. 698/II-58, pp. 11–19, 2002.
9) T.C. Papanastasiou and A.G. Boudouvis. Flows of viscoplastic materials: models and computations. *Computers & Structures*, Vol. 23, pp. 677–694, 1997.
10) K. Nakamura. Non-Newtonian Fluid Mechanics. Corona Publishing Co., Ltd., 1997.
11) K. Nagai and S. Ushijima. Computaional method with curvilinear coordinates for Bingham plastic fluids with free surfaces. *Annual Hounal of hydraulic Engineering, JSCE*, Vol. 54, pp. 1183–1188, 2010.

(Received March 9, 2010)